Storage influence in a combined biomass and power-to-heat district heating production plant

Nicolas Lamaison, Simon Collette, Mathieu Vallée, Roland Bavière

Storage Influence in a Combined Biomass and Power-to-Heat District Heating Production Plant

Nicolas Lamaison[1,2*], *Simon Collette*[1, 2], *Mathieu Vallée*[1, 2] *and Roland Bavière*[1,2]

[1] *Univ. Grenoble Alpes, INES, F-73375 Le Bourget du Lac, France*
[2] *CEA, LITEN, 17, Rue des Martyrs, F-38054 Grenoble, France*

Abstract

The increasing penetration of wind and solar electricity becomes challenging for grid operators. Interconnecting electrical and thermal networks through the Power-to-Heat concept brings flexibility to the electrical grid while supplying a significant renewable source to District Heating (DH). In the present paper, we study a DH production plant composed of a biomass generator, a heat-pump and a heat storage in the French energetic context. We assess the techno-economic performances of this system using Mixed Integer Linear Programming (MILP). A multi-objective parametric optimization method is applied to size the system using the available quantity of biomass, the maximum CO_2 content and minimum renewable energy ratio (REnR) of the heat production as ε-constraints. Our analysis shows that without strong constraints, heat pump and daily storage are used. For a limited amount of biomass available, we also show that investing in an inter-seasonal storage is necessary to reach high REnR. For comparisons, this energy system is also assessed with the Danish and German electric mix. We then verify the sizing stage results on the operational performances of a non-linear numerical simulator. With that methodology, it is possible to evaluate the impact of the MILP modelling level of detail on the obtained results. An error of 5.1% on the production trajectories is here obtained for a given system.

Keywords: ***District Heating, Power-to-Heat, Biomass, Storage, MILP, Model Predictive Control, Numerical Simulator***

Nomenclature

Greek Letters

Δt	Time step	[h]
η	Efficiency	[%]
σ	Number of cycles of the storage	[-]
τ	Discharging time at maximum power for storage	[h]

Latin Letters

c	Cost vector	[€/kWh] and [€/kW]
$CAPEX$	Capital Expenditure	[€]
CO_2^i	CO_2 content of the production of equipment i	[g/kWh]
COP	Coefficient of Performance of the Heat Pump	[-]
E	Energy	[kWh]
$EtoP_n$	Energy to Power normalized ratio	[-]
f_{cost}	Objective function	[€]
K_{loss}	Loss coefficient of the storage	[h^{-1}]
$LCOE$	Levelized Cost of Energy	[€/kWh]
LHV	Low Heating Value	[kWh/kg]
m	Mass of biomass	[kg]
N_{equ}	Number of heating equipment	[-]
N_{steps}	Number of time-steps considered	[-]
$OPEX$	Operational Expenditure	[€]
P	Power	[kW]
r	Ratio of minimum to maximum power of a given equipment	[-]
T_{life}	Lifetime of the equipment	[years]
T_{ON}	Minimum ON time of a given equipment	[h]
$REnR^i$	Renewable Energy Ratio of the production of equipment i	[-]
t_{actu}	Actualisation rate	[%]
Vol	Volume	[m^3]
X	Integer variable representing the startup of an equipment	[-]
x	Vector of decision variables	[-]
Y	Integer variable representing the ON/ OFF state of an equipment	[-]

Acronyms

DH	District Heating
DHN	District Heating Network
DHW	Domestic Hot Water
$MI(N)LP$	Mixed Integer (Non) Linear Programing
MOO	Multi Objective Optimization
MPC	Model Predictive Control
$R\&R$	Renewable and Recovery
$REnR$	Renewable Energy Ratio

Subscripts and superscripts

$_{ch/disch}$	Charge/discharge of the storage
$_{el/th}$	Electrical/Thermal based
$_{invest}$	Investment
$_{load}$	DHN heat load
$_{maint}$	Maintenance
$_{max}$	Maximal value
$_{max,int}$	Intermediate maximal value
$_{min}$	Minimal value

$prod$	Production
$start$	Starting up of equipment
bio	Biomass boiler
c	Constraint
hp	Heat pump
$mix,elec$	Electric mix
st	Heat storage
T	Transpose of a matrix/vector
tot	Yearly based value

1. Introduction

In France, similarly to other European countries, 35% of the final energy consumption is devoted to space heating and domestic hot water preparation (DHW), which amounts to 665 TWh per year [1]. The French energy planning of 2016 [2] has identified District Heating Networks (DHN) as a solution to reduce the use of fossil energy to supply heat demands. Indeed, due to their ability to massively distribute renewable and recovery energies (R&R), DHN are expected to deliver 5 times more R&R in 2030, to reach about 40TWh. Similarly, the Heat Roadmap France [3] recommends that DHN should cover up to 25% of the heat demand by 2050 while its current share is only 6%.

In parallel, the concept of 4th Generation District Heating [4, 5] emphasizes the need to interconnect DHNs to the power grid, as a way to provide the flexibility required for a broader integration of intermittent renewable energies [6]. In France, while combined Heat and Power (CHP) is limited by the rather low price of nuclear-based electricity, this integration will then be first driven by Power-to-Heat (PtoH) [7]. Indeed, combining PtoH with thermal storage provides a cheap and efficient form of storing excess renewable power [8].

At the same time, and contrarily to other EU countries, biomass is expected to play a major role and reach 50% in the French DHN mix by 2030 [9]. It is worth mentioning that the number of biomass-based DHN in France has significantly grown over the last 10 years, mainly because of financial incentives. It is now estimated that about 500 DHN [10] are using biomass in their energy mix. However, biomass must always be considered as a limited resource, unevenly distributed and affected by transportation constraints [11]. Moreover, its renewable nature depends on its usage rate.

In this paper, we study the optimal sizing of a DHN production plant combining PtoH, biomass and storage in the French context. In particular, we consider the influence of several parameters on the need for different thermal energy storage sizes, from small water tanks to large inter-seasonal storages. We consider only water-based storage at the production side, although other technologies as well as storing heat at building level or in the network itself could be considered at later stages [12].

According to the background and literature review, the paper is then structured as follows. In Section 2, we provide an overview of the state-of-the-art on similar systems, as well as on the typical sizing methodologies used for such studies. Section 3 presents the studied production plant, the methodology adopted in this study, which combines an optimal sizing stage with a sizing validation stage. In Section 4, we detail the Mixed-Integer Linear Programming (MILP) model used for optimal sizing definition, its implementation and the results obtained under various annual constraints. Section 5 aims at validating the designed system by assessing its operational performance through simulation with a numerical simulator of the system in order to calculate the possible deviations from the optimal sizing calculation. In Section 6, we conclude and propose some perspectives.

2. State-of-the-art

2.1. Smart energy systems combining biomass, power-to-heat and thermal storage capacities

As pointed out by Kwon and Ostergaard [13], it seems rather evident that the biomass resource will be subjected to a sever supply stress in the coming years with for example better purposes elsewhere in the energy systems. Thus, methodologies that cannot account for the limited availability of this resource are inappropriate in practice.

The on-going work of Koch and Gaderer [13] addresses the intelligent controlling of a system combining a solid-driven biomass cogeneration heat plant (CHP) and PtoH with heat storage capacities enables a DHN to contribute to the electricity and balancing market, thereby increasing the overall system efficiency. In their recent work, a conceptual approach for studying the flexibility-oriented sizing of such system is described. Their methodology relies on a set of simulated scenarios ran on a numerical simulator but does not account for annual constraints limiting.

The work of Ostergaard et al. [15] investigates the transition from biomass-based DHN to heat pump and storage based DHN from a business and socio-economic point of view. It is highlighted that even though the heat pump and storage system is interesting especially thanks to the flexibility it offers, it seems rather limited from an economical point of view. As pointed out in next section, it seems that the rule-based operation they used to perform their analysis is not harnessing the full potential of such energy system, thus reducing its economic benefit.

In the holistic approach of DHN production plant of Dahl et al. [14], applied in the Danish energetic context, it is shown that when the fossil-based resources are limited, investing in large-scale heat pumps and heat storages is desirable, phasing-out the use of CHPs, with only a slight increase of system cost.

As noticed previously, while biomass boiler is generally used as CHP throughout European DHNs, biomass boilers are seldom used as CHP in the French energetic context because of the largely nuclear-based electrical production. Even though there is a high potential to combine the numerous available biomass boilers with PtoH and storage capacities, no studies dealing with such a system in the French context could be found in the open literature.

2.2. Optimal sizing methodologies

Concerning the sizing approach, traditional methods use either duration curves and linear cost characteristics as explained in Frederiksen and Werner [17] or dynamic simulation tools with rule-based control strategies as used by Ostergaard et al. [15] for combined heat pump and storage operation and Lund et al. [17] for distributed small-scale CHP plants. Both methods are not capable of optimally sizing production plants when resources exhibit highly variable costs, e.g. electricity, or when the plant has storage capacities. Moreover, adding annual constraints, such as CO_2 or renewable contents of the production or limited annual quantity of a given resource, e.g. biomass, to these methods is complex and time consuming since iterative methods have to be used. On the other hand, operational performances of complex energy systems can be significantly underestimated when rule-based control is used. This has been shown by the work of Giraud et al. [19] in the field of DHN operation and Dufo-Lopez et al. [20] in the field of hybrid photovoltaics-based system operation. These elements explain why the results obtained using both aforementioned methods can be said sub-optimal.

In comparison, since their introduction by Grossmann [21] for the study of energy systems, Mixed Integer Linear Programming (MILP) methods have been used successfully in numerous energy studies, e.g. for CO2 network and power to gas [22], process integration [23], refrigeration systems [24] and solar assisted heat pumping [25]. A detailed review of optimization studies in energy systems dealing with electricity, heating and cooling by Ünal et al. [26], highlights the extensive growing usage of MILP approach in the community. The advantages of such a method are the following: i) the close relation of a MILP formulation to the physical equations, which facilitates the expression of realistic models, ii) the reasonable computational time, and iii) the guarantee of finding global optimality, which especially ensures the perfect reproducibility of results when performing comparisons.

The main drawback is the requirement of using only linear or quasi-linear models. When dealing with energy systems, nonlinear behaviors are plentiful, e.g. fluid transportation and temperature dependent efficiencies, leading to strong approximation of MILP approaches in some cases. The latter is the reason why some authors have investigated global optimizers such as genetic algorithms, e.g. for trigeneration systems [19, 20] or Mixed Integer Non Linear Programming (MINLP), e.g. for multi-period CHP plants [29]. Both strategies tend to be computationally costly and thus not appropriate in sizing stage. Moreover, in both strategies, the available algorithms are not robust enough and may converge to local, instead of global, optimum.

Instead of trying to overcome the main drawback of MILP programming, i.e. the linear approximation of all the physical phenomena, the present study uses a detailed non-linear numerical simulator of the system to validate and/or update the results from the MILP-based sizing. That innovative methodology allows to incrementally add complexity to the sizing MILP until satisfactory operation of the detailed numerical simulator is achieved. We present the adopted methodology in the next section of the present paper.

3. Methodology

The present section starts with the presentation of the studied heat production plant. An overview of the methodology used throughout this study is then addressed. The boundary conditions and input data are presented in sequence. Finally, the performance indicators we used are listed.

3.1.System description

Following the assessment presented in section 1, the present paper studies the production plant presented in Figure 1. It comprises a biomass boiler, a heat pump as PtoH element and a thermal storage in parallel arrangement. It also comprises a back-up gas boiler in serial arrangement just before the exit of the plant so that the demand is always satisfied even during peak or maintenance periods.

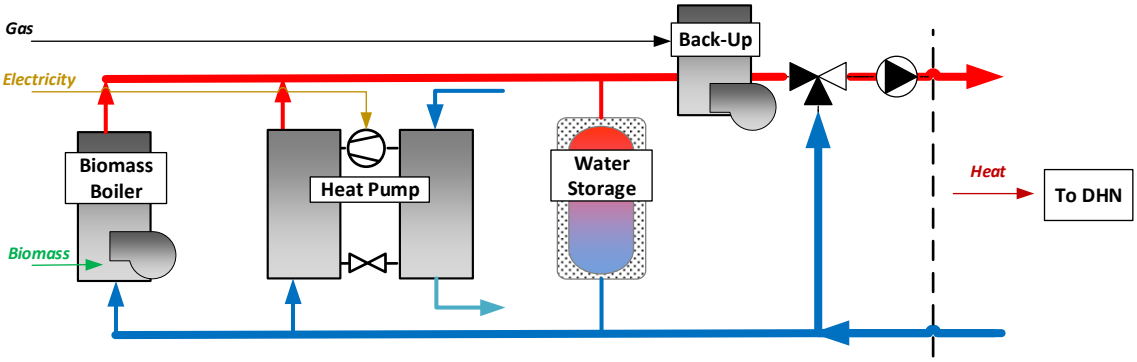

Figure 1: Studied combined Biomass and PtoH production plant

3.2.Overview

Figure 2 gives an overview of the methodology used in this work, which combines an optimal sizing stage with a sizing verification stage.

Starting from given input data (investment costs, efficiencies, technical limitations) and boundary conditions (DHN load, variable costs), optimal sizing of the system is firstly performed with quasi-linear models (Stage 1 in Figure 2). For the latter, the decision variables are gathered in two groups, i.e. the operational ones that require a value at each time step (e.g. Power level of each equipment) and the sizing ones that have a unique value (e.g. size of the storage). For this sizing stage, a single optimisation is performed with a fixed horizon of 1 year. The results are then extrapolated over the life time of the production plant T_{life}, set in the present study at 20 years. The results of this optimal sizing stage are i) the sizing of the system and ii) the operational variables trajectories and indicators (presented in section 3.4).

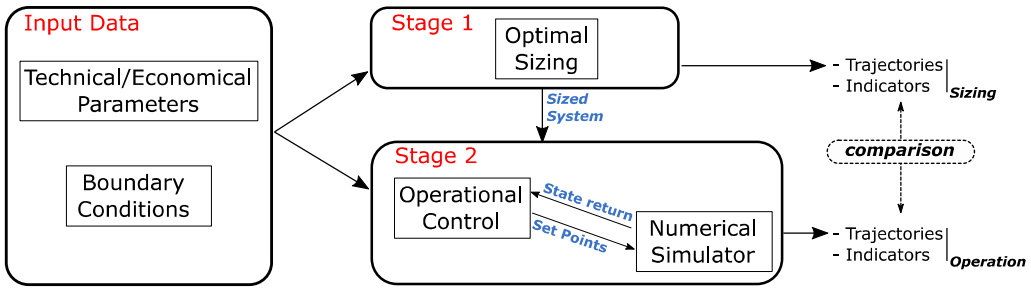

Figure 2: Overview of the methodology used in the present study

Secondly, the sizing is verified in operation (Stage 2 in Figure 2) with the same given input data and boundary conditions. For that stage, the sizing parameters are fixed and used by the operational control module. The latter uses a Model Predictive Control (MPC) algorithm to calculate the operational variables trajectories on a receding horizon. Results of this calculation are used as set points for a numerical simulator of the system, i.e. a detailed thermal-hydraulic and non-linear model of the production plant. The outputs of this numerical

simulator, i.e. the operational variables trajectories and indicators, are compared to the ones obtained during the sizing stage to validate the sizing.

The same boundary conditions are considered for the optimal sizing, the operational control and the numerical simulator. The latter means for example that the load curve considered during the sizing stage is the same as the one considered for the numerical simulator, which is representing real life operation. The latter thus represents idealistic conditions with no uncertainties in the prediction models. It is worth mentioning that the present methodology is able to deal with uncertainties on the boundary conditions.

While studies dealing with the sizing of energy systems generally consider only the sizing based on a single MILP optimization using an horizon of 1 year (Stage 1 in Figure 2), the present work uses a non-linear numerical simulator to both verify the sizing and evaluate more realistically the operational performances (Stage 2 in Figure 2).

3.3.Boundary conditions and input data

This section presents the main boundary conditions and input data used for both the sizing and the validation stages in sections 4 and 5. Part of this data is highly dependent on the country, so specific cases for France, Denmark and Germany have been considered (see section 3.3.2). Denmark and Germany energetic contexts are here used as comparisons with the French case.

3.3.1. Country-independent data

Electricity Price.

The electricity price considered is composed of a constant part, representing taxes and transportation, and a variable part, i.e. the electricity exchange price. In France, the constant part is approximately equal to 45€/MWh. As for the variable price, it was extracted from the 2017 EPEX-Spot database [30], the most used electricity exchange market in Europe. It is worth mentioning here that the same electricity costs were considered in all the energetic contexts. In reality, even though the day-ahead market prices are similar [30], that assumption is incorrect since transportation and taxes are different. However, this assumption is acceptable here since i) the error introduced in the electricity cost is in the order of 15% and ii) the objective here is to compare the electric mix influence.

Network Load

We generated a representative load using a tool [31] which provide an hourly profile demand of a DHN accounting for space heating, DHW preparation and network losses. We consider 3000 equivalent dwellings, for which the distributed monthly consumption is presented in Table 1. We used weather data for the year 2017 in Chambéry in France, and we reconstructed cold water temperature (for DHW) and ground temperature (for DHN losses) using the models of Burch and Christensen [32] and Kasuda and Archenbach [33] respectively. A heating law was considered for the supply network temperature (65 to 95°C) and a return temperature of 45°C and 55°C was set respectively during heating (01/10 to 15/05) and non-heating seasons. DHN overall losses were assumed to represent 10% of the DHN supplied energy and were recalculated on an hourly profile using the ground temperature. The peak network load $P_{DHN,peak}$ and total demand $E_{DHN,yearly}$ obtained are respectively of 18 MW and 40.10^3 MWh. This leads to a $EtoP_n$ $(-)$ ratio, as defined by Equation (1), of 0.25, where 8760 is the number of hours composing a year and which is a typical value for DHN. The network load was considered the same in all the energetic-context so that the total heat demand was preserved.

$$EtoP_n = \frac{E_{DHN,yearly}}{P_{DHN,peak}} . \frac{1}{8760} = 0.25 \quad (1)$$

Table 1: Inputs monthly total and DHW consumption normalized respectively by the average monthly value of total and DHW consumption, for an equivalent dwelling in Chambéry area for the averaged building stock [31]

Jan	Feb	Mar	Apr	May	Jun	Jul	Aug	Sep	Oct	Nov	Dec	TOT
Monthly Consumption of the equivalent dwelling (normalized by the average monthly value)												
2.1	1.7	1.5	1.0	0.5	0.2	0.2	0.2	0.2	1.0	1.5	2.0	12.0
Monthly consumption of DHW(normalized by the average monthly value)												
1.13	1.11	1.04	1.04	1.0	0.93	0.80	0.74	0.98	1.0	1.09	1.14	12

Costs.

For the production plant heating equipment, Table 2 lists the values of the investment and production costs (c^i_{invest} and c^i_{prod}). For the heat pump, the production costs are obtained by dividing the sum of the variable and constant electricity prices by the heat pump coefficient of performance (COP), considered to be 3 in the present work.

$$COP = \frac{P^{hp}_{th}}{P^{hp}_{el}} \quad (2)$$

where the heat pump COP is defined as the ratio of thermal power provided to the DHN P^{hp}_{th} over the electrical consumption of the heat pump P^{hp}_{el}.

Concerning the storage, $c^{st}_{invest_E}$ and $c^{st}_{invest_P}$ respectively the investment related to the energy and power sizing, are obtained from a study dedicated to PtoH and storage in France [7] and from the work of Eames et al. [34]. $c^{st}_{invest_E}$ is calculated using a two-parts piecewise linear formulation, in which the bottom part relates to low capacity tank (3 €/kWh$_{th}$) while the upper part relates to high capacity pit storages (0.8 €/kWh$_{th}$). For $c^{st}_{invest_P}$, it is set to 4.6 €/kW.

Input data.

Table 2 contains other data such as the ratio of minimum power to maximum power r^i of all the heating equipment. The latter aims at representing the technical limits of the different components which play a decisive role in the way the production plant is conducted (e.g. switch off of the biomass boiler when the load is below the minimum technical limit). The values were averaged from various manufacturers catalogues. The last two rows of Table 2 are related to the CO_2 content and Renewable Energy Ratio (REnR) of each equipment.

Table 2: Parameter values for the production plant equipment

Parameters	Unit	Biomass Boiler	Heat Pump	Back up Gas Boiler
c^i_{prod}	€/kWh$_{th}$	0.03 (Ref.[35])	0.015 to 0.082 (Ref. [30])	0.065 (Ref.[35])
c^i_{invest}	€/kW	940 (Ref. [36])	300 (Ref. [7])	100 (Ref. [36])
T^i_{on}	h	10 (Ref. [7])	1 (Ref. [7])	1 (Ref. [7])
r^i	-	0.4	0.1	0
CO^i_2	g/kWh$_{th}$	24 (Ref. [37])	21 to 894 (variable and context-dependent, see section 3.3.2)	240 (Ref. [37])
$REnR^i_{th}$	%	100	7 to 96 (variable and context-dependant, see section 3.3.2)	0

3.3.2. Country-dependent data

Although the study focuses on the French context, we also performed a comparison with the Danish and German contexts, especially regarding the CO_2 content and REnR of electricity. Figure 3 presents the CO_2 emissions in g/kWh$_{el}$ of the electricity production for the three countries. It was obtained using the annual electricity production planning from the European Network of Transmission System Operators for Electricity database of year 2017 [38]. In order to convert these profiles to CO_2 emissions in g/kWh$_{th}$ of the heat pump production, the values are divided by the COP of the heat pump.

Similarly, Figure 4 presents the REnR of the electricity production for the year 2017 in France, Germany and Denmark. In order to convert these profiles to the REnR of the heat pump production, Equation (3) must be used.

$$REnR_{th}^{hp}(t) = \frac{REnR_{el}^{mix,elec}(t)}{COP} + \frac{COP - 1}{COP} \quad (3)$$

where $REnR_{th}^{hp}(t)$ is the thermal renewable energy ratio of the heat pump, $REnR_{el}^{mix,elec}(t)$ is given by Figure 4.

The main conclusions to draw from the profiles of Figure 3 and Figure 4 are the following: i) France exhibits both a low CO_2 content but also a low REnR because of its nuclear-based electrical production, ii) in Denmark, the very-intermittent wind power backed up by coal-fired power plant leads to highly variable CO_2 content and REnR both at much larger values than in France, and iii) Germany lies in between the French and Danish contexts, since its electricity production exhibits a significant share of photovoltaics also backed-up by coal-fired power plants.

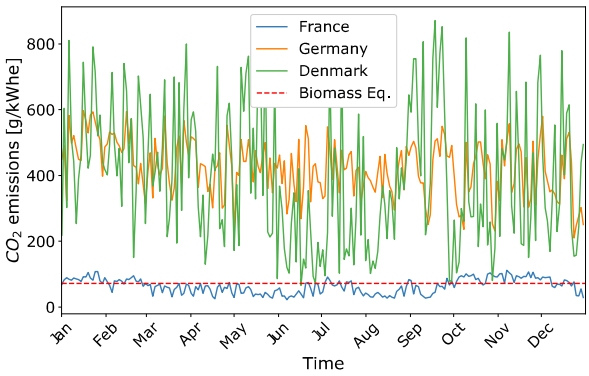

Figure 3: CO_2 emissions of the electrical production in g/kWhe for the year 2017 in France, Germany and Denmark. The equivalent Biomass CO_2 emissions per kWhe is calculated accounting for a factor of 3 (COP of the heat pump)

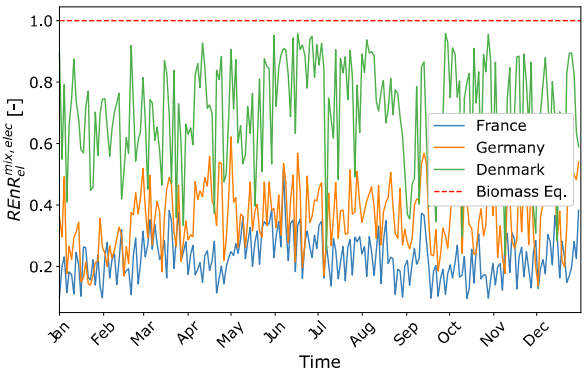

Figure 4: REnR of the electrical mix production for the year 2017 in France, Germany and Denmark. The Biomass REnR is considered to be 1.

3.4.Indicators

The main indicator used here is the Levelized Cost of Energy (LCOE), calculated with Equation (4) in €/kWh$_{th}$. It represents the average minimum price at which the produced heat must be sold in order to break-even over the lifetime of the production plant T_{life}.

$$LCOE = \frac{c_{tot}}{\sum_{y=1}^{T_{life}} \frac{\sum_{t=1}^{N_{steps}} P_{load}(t).\Delta t}{(1+t_{actu})^{y-1}}} \quad (4)$$

Where $P_{load}(t)$ [kW] represents the DHN heat load at time step t (see section 3.3.1), Δt [h] and N_{steps} represents respectively the time step and the number of time steps, t_{actu} [%] is the annualization factor (set to 5%), c_{tot} is the sum of the capital expenditure (CAPEX) and the annualized operating expenditure (OPEX) over the life time of the equipment T_{life}. c_{tot} is calculated using Equation (5).

$$c_{tot} = c_{invest} + \sum_{k=1}^{T_{life}} \frac{1}{(1+t_{actu})^{k-1}} (c_{prod} + c_{start} + c_{maint}) \quad (5)$$

Where c_{invest}, c_{maint}, c_{prod}, and c_{start} are respectively the investment, maintenance, production and starting costs. These terms are further detailed in the next section.

Two other indicators are used, i.e. the yearly thermal REnR and CO_2 content of the heat production, as defined respectively in Equations (6) and (7). It is worth mentioning that from now on, all the decision variables for the optimal sizing or the operational control will be highlighted in bold font to ease the reading of the equations.

$$CO_2^{tot} = \frac{\sum_{t=1}^{N_{steps}} \sum_{i=1}^{N_{equ}} CO_2^i . \boldsymbol{P^i}(\boldsymbol{t}) . \Delta t}{\sum_{t=1}^{N_{steps}} P_{load}(t) . \Delta t} \quad (6)$$

$$REnR_{th}^{tot} = \frac{\sum_{t=1}^{N_{steps}} \sum_{i=1}^{N_{equ}} REnR_{th}^i(t) . \boldsymbol{P^i}(\boldsymbol{t})}{\sum_{t=1}^{N_{steps}} P_{load}(t)} \quad (7)$$

Where the CO_2^i and $REnR_{th}^i$ represent the CO_2 content and the thermal REnR of the production by the different N_{equ} equipment. Their values were listed in Table 2. Additionally, $\boldsymbol{P^i}(t)$ [kW], represents the power value at time step *t* of equipment *i.* From now on, the REnR will always be the thermal one.

4. Optimal System Sizing

The present section deals with the sizing problem formulation and implementation of the optimal sizing presented in Figure 2 of the previous section. The obtained results are then discussed.

4.1. Base MILP problem formulation

At the optimal sizing stage, we formulate a MILP problem, with an objective to find the vector of decision variables $\boldsymbol{x}^T = (\boldsymbol{x_1}, \dots \boldsymbol{x_j}, \boldsymbol{x_{j+1}}, \dots, \boldsymbol{x_n})$ solution of the problem of Equation (8), $\boldsymbol{x}$ being composed of continuous $(1, \dots, j)$ and integer $(j+1, \dots, n)$ variables.

$$\begin{aligned} &\min_x f_{cost} = c^T.\boldsymbol{x} \\ &with \begin{cases} LHS \leq A.\boldsymbol{x} \leq RHS \\ l_b \leq \boldsymbol{x} \leq u_b \end{cases} \end{aligned} \tag{8}$$

where c [n] is a vector of cost, A[m x n], LHS[m] and RHS[m] are respectively the matrix and vectors of linear constraints, and l_b [n] and u_b [n] are respectively the lower and upper bounds vector for the decision variables.

4.1.1. Objective Function

The problem objective in Equation (8) is the minimization of the cost function f_{cost} which is calculated with Equation (9) (as c_{tot} in Equation (5)).

$$f_{cost} = c_{tot} = c_{invest} + \sum_{k=1}^{T_{life}} \frac{1}{(1+t_{actu})^{k-1}} (c_{prod} + c_{start} + c_{maint})$$

$$\begin{cases} c_{invest} = c^{st}_{invest_E}.\boldsymbol{E^{st}_{max}} + c^{st}_{invest_P}.\boldsymbol{P^{st}_{max}} + \sum_{i=1}^{N_{equ}} c^i_{invest}.\boldsymbol{P^i_{max}} \\ c_{maint} = \sum_{i=1}^{N_{equ}} c^i_{invest}.\boldsymbol{P^i_{max}}.0.01 \\ c_{prod} = \sum_{t=1}^{N_{steps}} \sum_{i=1}^{N_{equ}} c^i_{prod}.\boldsymbol{P^i}(t).\Delta t \\ c_{start} = \sum_{t=1}^{N_{steps}} \sum_{i=1}^{N_{equ}} c^i_{start}.\boldsymbol{X^i}(t) \end{cases} \tag{9}$$

Where c_{invest}, c_{maint}, c_{prod}, and c_{start} are respectively the investment, maintenance, production and starting costs. For confidentiality reasons, it is generally rather complicate to get correct values for the starting costs c^i_{start}. In order to prevent incorrect optimization because of too high starting costs, the latter have been set to a negligible value and are only used to write the constraint on the minimum ON time of the component, as explained in section 4.1.4. $\boldsymbol{E^{st}_{max}}$ [kWh$_{th}$], $\boldsymbol{P^{st}_{max}}$ [kW] and $\boldsymbol{P^i_{max}}$ [kW] represents the sizing values of respectively the maximum energy content of the storage, the maximum power of the storage, the maximum power of equipment i, and $\boldsymbol{X^i}(t)$ is an integer variable equal to 1 when the equipment just started and 0 otherwise.

4.1.2. Modelling assumptions

In the sizing MILP model, the following assumptions were made in order to have a tractable problem:

- The COP of the heat pump does not vary with the temperature or power levels of the heat pump;
- Thermal stratification is not accounted for in the storage;
- Resource costs are not affected by the operation of the DHN. In reality, the electricity or biomass costs may be influenced by the large consumptions of many such production plants;
- In the sizing stage, the heat loss of the storage are considered null because a constant value (required for the linear models) would give misleading results since the losses should be dependent on the size

of the storage which is a decision variable. Heat loss are however accounted for in operation in section 5.

4.1.3. Equality Constraints

Plant Energy Balance. As written in Equation (10), the total DHN heat load must be met at each time step t.

$$\sum_{i=1}^{N_{equ}} \boldsymbol{P^i}(\boldsymbol{t}) + \boldsymbol{P^{st}_{disch}}(\boldsymbol{t}) = \boldsymbol{P^{st}_{ch}}(\boldsymbol{t}) + P_{load}(t) \quad (10)$$

where $\boldsymbol{P^{st}_{disch}}(\boldsymbol{t})$ [kW] and $\boldsymbol{P^{st}_{ch}}(\boldsymbol{t})$ [kW] represent the discharging and charging power at time step t.

Storage Energy Balance. As written in Equation (11), a second energy balance can be written for the storage.

$$\frac{\boldsymbol{E^{st}}(\boldsymbol{t}) - \boldsymbol{E^{st}}(\boldsymbol{t-1})}{\Delta t} = \boldsymbol{P^{st}_{ch}}(\boldsymbol{t}) - \boldsymbol{P^{st}_{disch}}(\boldsymbol{t}) - K_{loss}.\boldsymbol{E^{st}}(\boldsymbol{t}) \quad (11)$$

where $\boldsymbol{E^{st}}(\boldsymbol{t})$ [kWh_{th}] is the energy content of the storage at time t, and K_{loss} [h^{-1}] is the overall heat loss coefficient. As explained beforehand, the latter is set to null in the sizing phase but is used during the operational validation in section 5.

4.1.4. Inequality Constraints

Equipment Power Capacity Bounds. The power supplied by each equipment is bounded by minimum and maximum values which are also decision variables, as shown in Equation (12).

$$r^i.\boldsymbol{P^i_{max}}.\boldsymbol{Y^i}(\boldsymbol{t}) \leq \boldsymbol{P^i}(\boldsymbol{t}) \leq \boldsymbol{P^i_{max}}.\boldsymbol{Y^i}(\boldsymbol{t}) \quad (12)$$

where $\boldsymbol{Y^i}(\boldsymbol{t})$ is an integer variable representing the ON or OFF state of the equipment i and r^i is the ratio between the minimum and maximum power of the equipment i. Because of the product of two decision variables, Equation (12) is nonlinear and must be rewritten using a big-M constraint formulation [39], introducing an intermediate variable $\boldsymbol{P^i_{maxint}}(t)$ representing a dynamic bound and M a very large number, as shown in Equation (13).

$$\begin{cases} \boldsymbol{P^i_{maxint}}(t) \leq M.\boldsymbol{Y^i}(t) \\ \boldsymbol{P^i_{max}} - M.\left(1 - \boldsymbol{Y^i}(t)\right) \leq \boldsymbol{P^i_{maxint}}(t) \leq \boldsymbol{P^i_{max}} \\ r^i * \boldsymbol{P^i_{maxint}}(t) \leq \boldsymbol{P^i}(t) \leq \boldsymbol{P^i_{maxint}}(t) \end{cases} \quad (13)$$

Storage Power Capacity Bounds. The power charged to or discharged from the storage at each time step is bounded by minimum and maximum values which are also decision variables, as shown in Equation (14).

$$\begin{cases} 0 \leq \boldsymbol{P^{st}_{ch}}(\boldsymbol{t}) \leq \boldsymbol{P^{st}_{max}}.(1 - \boldsymbol{Y^{st}}(\boldsymbol{t})) \\ 0 \leq \boldsymbol{P^{st}_{disch}}(\boldsymbol{t}) \leq \boldsymbol{P^{st}_{max}}.\boldsymbol{Y^{st}}(\boldsymbol{t}) \end{cases} \quad (14)$$

where $\boldsymbol{Y^{st}}(\boldsymbol{t})$ is an integer variable equal to 1 when the storage is discharging and 0 when it is charging, forbidding the storage to charge and discharge at the same time. Similarly to Equation (12), Equation (14) is nonlinear and must be rewritten using a big-M constraint formulation [39] similar to Equation (13).

Storage Energy Capacity Bounds. The energy content of the storage at each time step is bounded by a maximum value which is also decision variable, as shown in Equation (15).

$$0 \leq \boldsymbol{E^{st}}(\boldsymbol{t}) \leq \boldsymbol{E^{st}_{max}} \quad (15)$$

Minimum ON Time of the different equipment. In order to prevent the different equipment to start and stop too frequently, a minimum time of operation after a startup has been added as a constraint (see Equation (16) using a formulation similar to the one used by Yang et al. [40] for the so-called unit commitment problem in the electrical power production field.

$$\begin{cases} \boldsymbol{Y^i(t) - Y^i(t-1) \leq X^i(t) \leq Y^i(t)} \\ T_{on}^i . \boldsymbol{X^i(t)} \leq \sum_{k=1}^{T_{on}^i} \boldsymbol{Y^i(t+k-1)} \end{cases} \quad (16)$$

where T_{on}^i represents the minimum time ON of equipment i, and $\boldsymbol{X^i}$ and $\boldsymbol{Y^i}$ are integer decision variables already introduced beforehand and respectively representing the starting of the equipment and the state ON or OFF of the equipment.

4.1.5. Periodic Constraints

Additionally, some variables such as the energy content of the storage $\boldsymbol{E^{st}}$ and the ON/OFF state of the equipment $\boldsymbol{Y^i}$ are subjected to a periodic constraint stating that values at initial and final time steps are identical.

4.2. Annual ε-constraints

More than only minimizing the combined CAPEX and OPEX (see Equation (9)), other annual objectives faced by the DHN operator are added. Instead of implementing complex and computationally costly Multi-Objective Optimization (MOO), these objectives are added by the means of ε-Constraints as explained by Haymes et al. [41]. It is a simple approach to MOO but it requires a preselection of the values of these objectives prior to the optimization which might lead to unfeasible problem. The paragraphs below present the three different ε-Constraints considered in the present study.

4.2.1. Maximum amount of Biomass available

As discussed in section 1, biomass must be seen as a limited resource. Thus, an annual ε-constraint is added as shown in Equation (17)

$$\sum_{t=1}^{N_{steps}} \boldsymbol{P^{bio}(t)} . \Delta t \leq m_{max}^{bio} . LHV^{bio} . \eta^{bio} \quad (17)$$

where $\boldsymbol{P^{bio}(t)}$ [kW] is the power supplied by the biomass boiler at each time step, LHV^{bio}[kWh$_{th}$/kg] is the Low Heating Value of the biomass (set to 3.8 kWh$_{th}$/kg), m_{max}^{bio} [kg] is the amount of biomass available for one year, η^{bio} is the biomass boiler efficiency (set to 90%).

4.2.2. Maximum CO_2 content of the production

In general, one of the main advantage of DHNs compared to other heating solutions is to exhibit a low emission of CO_2. In France, the building envelope regulatory framework is for example relaxed if the DHN production to which the building is connected is below 50g/kW$_{th}$. The annual ε-constraint presented in Equation (18) thus forces the plant to operate below a predefined level of emission.

$$CO_2^{tot} \leq CO_2^{tot,c} \quad (18)$$

where CO_2^{tot} [g/kW$_{th}$] and $CO_2^{tot,c}$ [g/kW$_{th}$] are respectively the yearly CO_2 content of the plant production as defined respectively in Equation (6)and the yearly CO_2 content epsilon constraint of the plant production.

4.2.3. Minimum Renewable Energy Ratio (REnR) of the production

In France, DHN benefits from a reduced VAT if the REnR of their production is above 50%. Then, it is interesting to add an annual ε-constraint on the REnR, as shown in Equation (19).

$$REnR^{tot} \geq REnR^{tot,c} \quad (19)$$

where $REnR^{tot}$ [%] represents the yearly REnR of the plant heat production as defined in Equation (7), and $REnR^{tot,c}$ [%] is the REnR epsilon constraint of the production.

4.3. Optimal sizing implementation and solving

The optimization problem is implemented inside an in-house C++ based framework called PEGASE [42] which embeds MILP formulation capabilities based on the Eigen linear algebra library [44].

The overall sizing optimization problem is solved using CPLEX [43] for one year and a time-step of 2 hours. It leads to 35k continuous decision variables, 18k integer decision variables and 120k constraints. The latter leads to a computational time of 10 minutes for each optimization on an office laptop. Numerous optimizations were performed for different ε-constraints, as defined in section 4.2, and in different energetic contexts (French, Danish and German). The results are presented in next section.

4.4.Optimal sizing results

As discussed above, the focus is on the French energetic context for which the present heat production plant is meaningful. For comparisons purpose, the sizing is also performed with the REnR and CO_2 content of the electrical production from Denmark and Germany (see Figure 3 and Figure 4).

Figure 5 presents the LCOE-REnR Pareto front obtained for the three countries with no constraint on the CO_2 emissions and an available quantity of biomass equivalent to 36% of the total yearly load of the DHN. It is first observed that the studied production plant is intrinsically highly renewable (i.e. high x-axis values). Second, the LCOE increases with an increase of the minimal REnR constraint for France and Germany but not for Denmark. For the two former, the increase in LCOE highlights an increase of investment into a biomass boiler and a larger storage. For Denmark for which the electricity REnR is the highest (see Figure 4), the heat pump alone is sufficient even for these high constraints. Finally, it is worth mentioning that, for this available biomass constraint of 36% of the total DHN demand, France cannot reach REnR higher than 85% with its current electrical mix.

Figure 6 presents the LCOE-CO_2 content Pareto front for the three countries with no constraint on the available amount of biomass and a REnR constraint of 85%. That figure shows that the CO_2 constraint has no effect on the French case due to its decarbonized nuclear-based electricity. It is also shown that the higher is the CO_2 content of the electricity and the more it is required to invest in biomass and then in larger storage to cope with the CO_2 constraint.

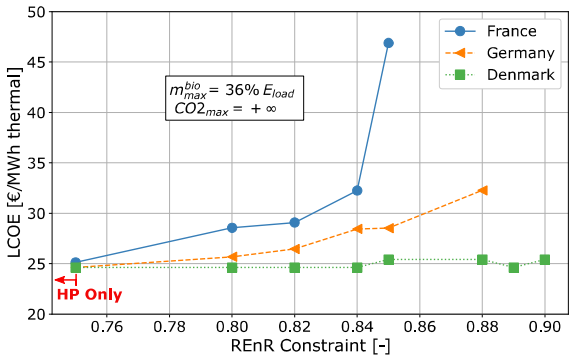

Figure 5: Pareto Front LCOE-REnR for France, Denmark and Germany with no ε-constraint on the CO_2 and an available mass of biomass equivalent to 36% of the total DHN load. HP only scenario is highlighted.

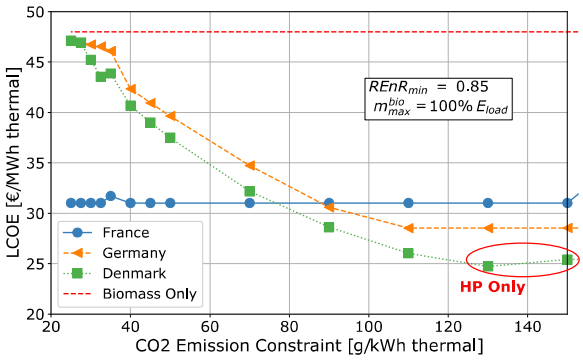

Figure 6: Pareto Front LCOE-CO_2 emission for France, Denmark and Germany with an ε-constraint on the REnR of 85% and an infinite mass of biomass available. Biomass only and HP only scenario are highlighted.

Figure 7 presents the LCOE-REnR Pareto front obtained in France for two different levels of availability for biomass and no constraint on the CO_2 content (which has no effect, see Figure 6). It shows how increasing the availability of biomass affects the Pareto front. Two main conclusions can be drawn from this figure: i) the LCOE increases almost linearly with the REnR constraint until a transition point at which it rapidly increases, and ii) increasing the available quantity of biomass first displaces this transition point towards higher REnR and second, allows reaching feasible solution at higher REnR constraint (85% for 36% biomass available and 90% at 58% biomass available).

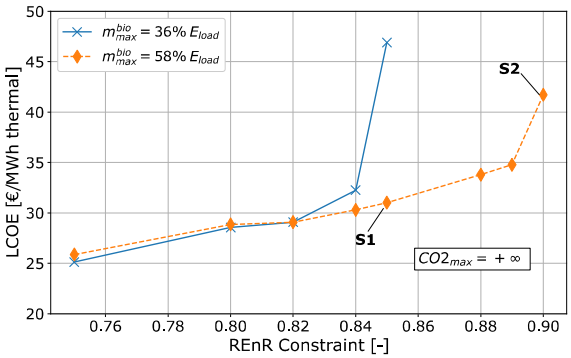

Figure 7: Pareto Front LCOE-REnR for France with no ε-constraint on the CO_2 and a variable available mass of biomass. S1 and S2 systems have been selected for comparisons

This transition point is linked to the need of drastically increasing the capacity of the storage. The latter is underlined by studying more specifically two different sizing S1 and S2, located in Figure 7. The main characteristics of these two systems are listed in Table 3. It is shown that they are not that different in terms of heat pump and biomass capacities. However, storages characteristics are completely different with S2 highlighting a clear inter-seasonal behavior compared to S1: i) 40 times higher capacity, ii) 2 cycles σ^{st} (see Equation (20)) instead of 48, and iii) a maximum discharge time at maximum power τ^{st} (see Equation (21)) of more than 500 hours. That inter-seasonal behavior of S2 compared to the behavior of sizing S1 is illustrated in the yearly profiles of Figure 8 (S1) and Figure 9 (S2) where the remaining discharge time at maximum power $\left(\tau^{st} = \frac{E^{st}}{P^{st}_{max}}\right)$ is shown. Interestingly, the weekly profiles of Figure 10 (S1) and Figure 11 (S2), shown for a week in March, are very similar. It is worth mentioning that both sizing do not consider any back-up capacity in their investments.

$$\sigma^{st} = \frac{\sum_{t=1}^{N_{steps}} \boldsymbol{P^{st}_{ch}}(t).\Delta t}{\boldsymbol{E^{st}_{max}}} \quad (20)$$

$$\tau^{st}_{max} = \frac{\boldsymbol{E^{st}_{max}}}{\boldsymbol{P^{st}_{max}}} \quad (21)$$

Table 3: Differences between the two systems of Figure 7

SIZING	S1	S2
$\boldsymbol{m^{bio}}$ [$\%\boldsymbol{E_{load}}$]	41%	58% (contraint)
$\boldsymbol{P^{bio}_{max}/P_{load,max}}$ [-]	0.34	0.44
$\boldsymbol{P^{HP}_{max}/P_{load,max}}$ [-]	0.46	0.40
$\boldsymbol{P^{st}_{max}/P_{load,max}}$ [-]	0.49	0.74
$\boldsymbol{E^{st}_{max}/E^{st}_{max,S1}}$ [-]	1	40
$\boldsymbol{\sigma^{st}}$ [-]	48	2
$\boldsymbol{\tau^{st}_{max}}$ [$\boldsymbol{h}$]	20	537

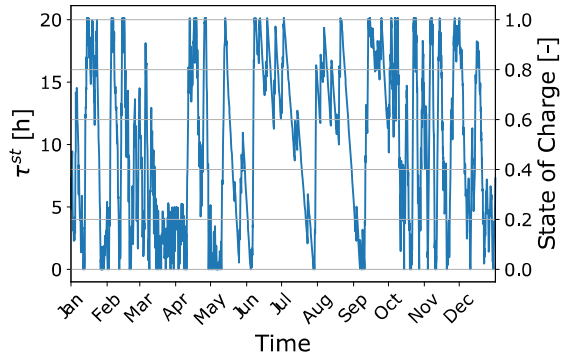

Figure 8: Yearly behavior of the storage in system S1

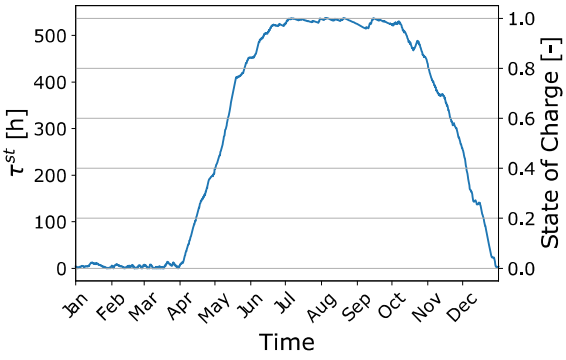

Figure 9: Yearly behavior of the storage in system S2

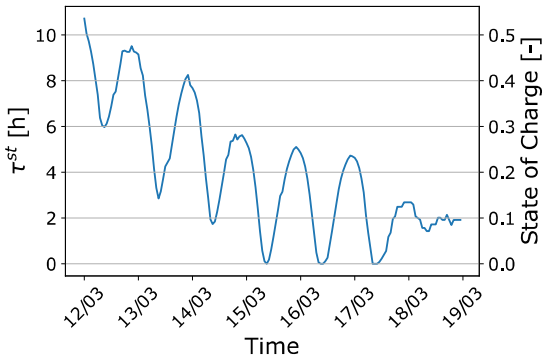

Figure 10: Weekly behavior of the storage in system S1

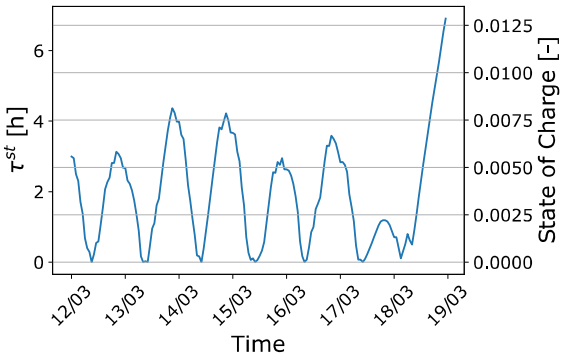

Figure 11: Weekly behavior of the storage in system S2

5. Sizing Verification through Operation

While the calculations that led to sizing S1 in Section 4 were performed with simple quasi-linear models, the purpose is now to evaluate the real performance of the production plant with a detailed non-linear simulator. As explained in the methodology presented in Section 3, the same input data and boundary conditions are applied to the simulator. The latter is controlled by a MPC using a modified MILP formulation from the one of Section 4. Implementation and solving of the production plant operational control are then presented. Finally, indicators of the more realistic performances are recalculated and compared to the ones obtained during the sizing-stage.

5.1.Operational MILP

The MILP formulation for the operation is slightly different than the one presented in Section 4, which dealt with both the sizing and the operation. Table 4 summarizes the differences between the sizing and the operational MILP formulations.

Table 4: Differences between the sizing and the operational MILP

MILP	Sizing	Operation
Decision Variables	Sizing + Operational	Operational Only
Annual Constraints	Yes	No
Power Bounds Constraints	Equ. (12) and (14) non linear	Equ. (12) and (14) linear
Objective function	$c_{invest} + c_{prod} + c_{start} + c_{maint}$	$c_{prod} + c_{start}$
Storage Loss	None	$K_{loss} = 0.009h^{-1}\ (2\%/day)$

5.2. Operational MILP implementation and solving

First, a detailed dynamic thermal-hydraulic model of the production plant has been implemented using Modelica programming language with the *Standard Modelica* and *DistrictHeating* [44] validated libraries. In this model, all the non-linear phenomena linked to the conservations of mass, momentum and energy are modelled using 1D unitary models of the production equipment and storage. The conservation equations are discretized using a finite volume scheme and relying on a staggered mesh for the fluid domain. The same approach is also used to model the "solid" domain where the heat conduction problem is solved.

For the production equipment, thermal inertia of the solid parts and heat losses to the ambient are respectively modelled using equivalent, i.e. lumped, thermal capacitance and heat transfer coefficient. Regarding the heat pump, a half-Carnot model has been used for the COP.

For the sensible storage, stratification is accounted for with the usage of a 1D vertical mesh for which axial conduction and heat losses through the lateral walls are considered for each discretized element.

Finally, to increase the time-step that can be used by the numerical integrator, the dynamics of the various PID controllers (e.g. supply temperature controller, power discharge controller …) are ignored by the simulator. This is done by formulating the regulators model in a continuous form. This simplifying assumptions is coherent with our objective to perform monthly to annual simulations.

Second, this Modelica model is used inside an in-house simulation framework called PEGASE [42] which, in addition to the MILP formulation capabilities already mentioned in Section 4.3, also embeds a master of co-simulation compatible with the FMI 2.0 standard.

Instead of doing a single optimization for a horizon of 1 year as in Section 4, we now realize an optimization every 15 minutes for the next 24h. With the MPC strategy, at each time step, the MILP problem is formulated and solved using the GLPK open source solver [45] and the simulator uses the outputs of the MPC strategy, sending back to the control module state returns such as the level of energy in the storage.

At a time step of 15 minutes, each operational optimization problem has about 700 continuous decision variables, 360 integer decision variables and 2400 constraints. On an office laptop, the latter leads to a computational time of about 3 hours for a yearly simulation with an optimization every 15 minutes and a receding horizon of 24h (96 time steps). In other words, each time step requires approximately half a second.

5.3. Sizing verification and realistic operational performances

Figure 12 presents the profiles of biomass, heat pump and storage power and DHN load obtained with the numerical simulator. These results are in the forms of 2D maps where the x-axis represents the hours of the days and the y-axis represents the days of the year. In this way, each horizontal line corresponds to a daily profile while each vertical line corresponds to a yearly profile at a given hour of the day. For clarity reasons, the results focus on the January to May heating season only.

The two main conclusions to draw from these profiles are the following:

i) The biomass boiler is used as base load throughout the operation, since no sharp peaks of power are spotted;

ii) The heat pump and the storage have a combined action to cope with the demand peaks. First, the heat pump is used during the nights at low electricity cost hours to charge the storage. Second, the storage is discharged during the demand peaks in the mornings when electricity costs are high thus reducing the operational costs. It is interesting to notice that the charging of the storage takes place just before the discharge so that heat losses in the storage are limited.

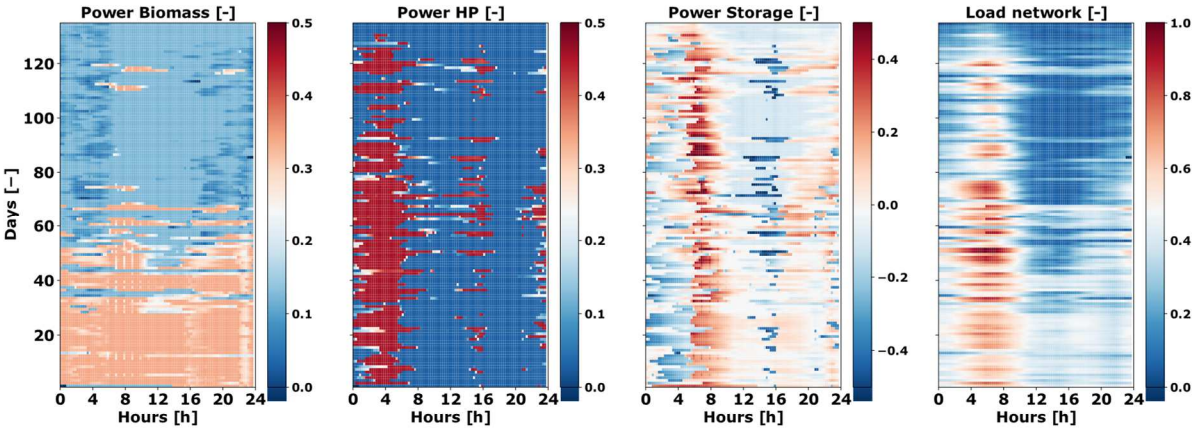

Figure 12: Biomass power, Heat Pump power, Storage power and DHN load for the January to May heating season operation of the S1 system. The results are normalized by the peak load of the DHN (18MW). A positive storage power means discharge while a negative one means charge.

We compared the power trajectories obtained during the sizing stage and the ones from Figure 12, i.e. the ones obtained during the operational control of the numerical simulator. While no back-up power (see Figure 1) was used during the sizing stage, 5.1% of the total heat demand was here supplied by the back-up gas boiler. The latter highlights that the assumptions considered for the sizing MILP of Section 4 such as the neglecting of temperature effects on COP, the stratification in the storage and the zero losses of the storage, led to an error of 5.1% on the energy mix.

Finally, we calculated in Table 5 the indicators listed in Section 3.4 for both the sizing and the operational stages. It is shown that the LCOE increases because of the storage losses and the use of the back-up. Also, the operational REnR is lower than what was expected during the sizing stage. The conclusion is that the results obtained during the sizing stage are too optimistic. The obtained differences highlight that a feedback between the operational results and the sizing results is still required and needs to be included in a future upgraded methodology. The later will be addressed in future studies.

Table 5: Indicators Comparisons between sizing and operational stage

MILP	Sizing	Operation
E (back-up) [%Eload]	0	5.1
LCOE [€/MWh$_{th}$]	31	33.6
REnR [%]	85	83.2

6. Conclusion and Outlook

In the present study, optimal sizing and operation of a DH production plant consisting of a biomass heat-only generator, a PtoH equipment and a heat storage was investigated in the French energetic context.

MILP formulation together with various ε-constraints were used to optimize the sizing. It was shown that the CO_2 constraint had no influence but that when high REnR were targeted with limited availability of the biomass, investments in inter-seasonal storage were required. For comparisons purposes, the Danish and German electrical mix were used to perform the optimal sizing. In these cases, the CO_2 constraint was proven to be the most decisive constraint.

One of the system sized in the French context was then tested in operation using a numerical simulator and a MPC strategy. The latter was shown to use at its best the association PtoH / storage by storing electricity in the form of heat when costs were low and restoring the heat at peak demands coincident with high electricity costs.

The methodology used here allows verifying the sizing by comparing indicators calculated with a simplified MILP formulation to indicators calculated with the simulated operation of a non-linear numerical simulator, keeping identical boundary conditions. It was here shown that a deviation of 5% of the energy mix was obtained which led to errors on the LCOE and REnR content of 2.6€/MWh, and 1.8% respectively.

With the take-off of heat pump technology on district heating in France where a lot of medium-sized DHNs are already based on biomass, it is here proven that the combination of both associated to some storage capabilities represents an attractive solution.

Addressing the topic of sizing in a more holistic approach is a future ambition with the addition of cogeneration plant, simultaneous heating and cooling heat pumps and cold storage to respond to electric, heat and cold demands. Regarding MPC optimization, future studies will include multi-horizons optimization in the methodology in order to be able i) to account for annual constraint, ii) properly optimize the operation of an inter-seasonal storage and iii) minimize the observed deviations between the sizing and operational stages.

References

[1] European Comission, “An EU Strategy on Heating and Cooling,” Brussels, Feb. 2016.

[2] République Francaise, “Programmation Pluriannuelle de l’Energie,” *Journal Officiel de la République Française*, Oct-2016.

[3] S. Paardekooper *et al.*, “Heat Roadmap France: Quantifying the Impact of Low-Carbon Heating and Cooling Roadmaps,” 2018.

[4] H. Lund *et al.*, “4th Generation District Heating (4GDH),” *Energy*, vol. 68, pp. 1–11, Apr. 2014.

[5] H. Lund *et al.*, “The status of 4th generation district heating: Research and results,” *Energy*, vol. 164, pp. 147–159, Dec. 2018.

[6] A. Vandermeulen, B. van der Heijde, and L. Helsen, “Controlling district heating and cooling networks to unlock flexibility: A review,” *Energy*, vol. 151, pp. 103–115, May 2018.

[7] “Étude de valorisation du stockage thermique et du power-to-heat,” ADEME, Nov. 2016.

[8] H. Lund *et al.*, “Energy storage and smart energy systems,” *Int. J. Sustain. Energy Plan. Manag.*, vol. 11, pp. 3–14, 2016.

[9] SNCU, “Enquête annuelle sur les réseaux de chaleur-restitution des statistiques 2014,” 2015.

[10] AMORCE, “Les réseaux de Chaleur au bois (rapport 2016 - données 2014),” RCT 42, Décembre 2016.

[11] K. Ericsson and L. J. Nilsson, “Assessment of the potential biomass supply in Europe using a resource-focused approach,” *Biomass Bioenergy*, vol. 30, no. 1, pp. 1–15, Jan. 2006.

[12] M. Leśko, W. Bujalski, and K. Futyma, “Operational optimization in district heating systems with the use of thermal energy storage,” *Energy*, vol. 165, pp. 902–915, Dec. 2018.

[13] K. Koch and M. Gaderer, “Intelligent Controlling of Power Driven Solid Biomass CHP Plants in Flexible District Heating With a Seasonal Heat Storage And a Power-To-Heat Component,” presented at the The Future Role of Thermal Energy Storage in the UK Energy System: An Assessment of the Technical Feasibility and Factors Influencing Adoption, Copenhagen, Denmark, 2018.

[14] M. Dahl, A. Brun, and G. B. Andresen, “Cost sensitivity of optimal sector-coupled district heating production systems,” *Energy*, vol. 166, pp. 624–636, Jan. 2019.

[15] P. A. Østergaard, J. Jantzen, H. M. Marczinkowski, and M. Kristensen, "Business and socioeconomic assessment of introducing heat pumps with heat storage in small-scale district heating systems," *Renew. Energy*, vol. 139, pp. 904–914, Aug. 2019.
[16] P. S. Kwon and P. A. Østergaard, "Priority order in using biomass resources – Energy systems analyses of future scenarios for Denmark," *Energy*, vol. 63, pp. 86–94, Dec. 2013.
[17] S. Frederiksen and S. Werner, *District Heating and Cooling*. Professional Pub Serv, 2013.
[18] H. Lund, G. Šiupšinskas, and V. Martinaitis, "Implementation strategy for small CHP-plants in a competitive market: the case of Lithuania," *Appl. Energy*, vol. 82, no. 3, pp. 214–227, Nov. 2005.
[19] L. Giraud, M. Merabet, R. Baviere, and M. Vallée, "Optimal control of district heating systems using dynamic simulation and mixed integer linear programming," in *Proceedings of the 12th International Modelica Conference, Prague, Czech Republic, May 15-17, 2017*, 2017, pp. 141–150.
[20] R. Dufo-López, L. A. Fernández-Jiménez, I. J. Ramírez-Rosado, J. S. Artal-Sevil, J. A. Domínguez-Navarro, and J. L. Bernal-Agustín, "Daily operation optimisation of hybrid stand-alone system by model predictive control considering ageing model," *Energy Convers. Manag.*, vol. 134, pp. 167–177, 2017.
[21] I. E. Grossmann, "Mixed-integer programming approach for the synthesis of integrated process flowsheets," *Comput. Chem. Eng.*, vol. 9, no. 5, pp. 463–482, Jan. 1985.
[22] R. Suciu, L. Girardin, and F. Maréchal, "Energy integration of CO2 networks and power to gas for emerging energy autonomous cities in Europe," *Energy*, vol. 157, pp. 830–842, Aug. 2018.
[23] F. Marechal and B. Kalitventzeff, "Targeting the integration of multi-period utility systems for site scale process integration," *Appl. Therm. Eng.*, vol. 23, no. 14, pp. 1763–1784, Oct. 2003.
[24] M. R. Shelton and I. E. Grossmann, "Optimal synthesis of integrated refrigeration systems—I: Mixed-integer programming model," *Comput. Chem. Eng.*, vol. 10, no. 5, pp. 445–459, Jan. 1986.
[25] A. S. Wallerand, M. Kermani, R. Voillat, I. Kantor, and F. Maréchal, "Optimal design of solar-assisted industrial processes considering heat pumping: Case study of a dairy," *Renew. Energy*, vol. 128, pp. 565–585, Dec. 2018.
[26] A. N. Ünal, S. Ercan, and G. Kayakutlu, "Optimisation studies on tri-generation: a review: Optimisation studies on tri-generation: a review," *Int. J. Energy Res.*, vol. 39, no. 10, pp. 1311–1334, Aug. 2015.
[27] A. A. Rentizelas, I. P. Tatsiopoulos, and A. Tolis, "An optimization model for multi-biomass tri-generation energy supply," *Biomass Bioenergy*, vol. 33, no. 2, pp. 223–233, Feb. 2009.
[28] M. Burer, K. Tanaka, D. Favrat, and K. Yamada, "Multi-criteria optimization of a district cogeneration plant integrating a solid oxide fuel cell–gas turbine combined cycle, heat pumps and chillers," *Energy*, vol. 28, no. 6, pp. 497–518, May 2003.
[29] T.-M. Tveit, T. Savola, A. Gebremedhin, and C.-J. Fogelholm, "Multi-period MINLP model for optimising operation and structural changes to CHP plants in district heating networks with long-term thermal storage," *Energy Convers. Manag.*, vol. 50, no. 3, pp. 639–647, Mar. 2009.
[30] "EPEX-spot." [Online]. Available: https://www.epexspot.com. [Accessed: 21-Nov-2018].
[31] A.-S. Provent *et al.*, "Smart Grid Solaire Thermique: Rapport d'étude sur les réseaux de chaleur existants et les réseaux adaptés aux Eco-quartiers," ADEME, 1.1.1, Sep. 2013.
[32] J. Burch and C. Christensen, "Towards development of an algorithm for mains water temperature," in *Proceedings of the Solar Conference*, 2007, vol. 1, p. 173.
[33] T. Kasuda and P. R. Archenbach, "Earth Temperature and Thermal Diffusivity at Selected Stations in the United States," *ASHRAE Trans.*, no. 1, 1965.
[34] P. Eames, D. Loveday, V. Haines, and P. Romanos, "The Future Role of Thermal Energy Storage in the UK Energy System: An Assessment of the Technical Feasibility and Factors Influencing Adoption," UKERC, London, Nov. 2014.
[35] M. C. Soini, M. C. Bürer, D. P. Mendoza, M. K. Patel, J. Rigter, and D. Saygin, "Renewable Energy in District Heating and Cooling, A sector roadmap for REmap," IRENA, Mar. 2017.
[36] "Etude des coûts d'investissement et d'exploitation associés aux installations biomasse énergie des secteurs collectifs et industriels," ADEME, Mai 2015.
[37] "Energy and carbon conversions," Carbon Trust, 2008.
[38] "ENTSO-E." [Online]. Available: https://transparency.entsoe.eu/dashboard/show. [Accessed: 21-Nov-2018].
[39] I. Griva, S. Nash, and A. Sofer, *Linear and Nonlinear Optimization*, Society for Industrial Mathematics. 2008.
[40] L. Yang, C. Zhang, J. Jian, K. Meng, Y. Xu, and Z. Dong, "A novel projected two-binary-variable formulation for unit commitment in power systems," *Appl. Energy*, vol. 187, pp. 732–745, Feb. 2017.
[41] Y. Haimes, L. Lasdon, and D. Wismer, "On a bicriterion formation of the problems of integrated system identification and system optimization," *IEEE Trans. Syst. Man Cybern.*, vol. 1, no. 3, pp. 296–297, 1971.

[42] M. Vallée *et al.*, “An efficient co-simulation and control approach to tackle complex multi-domain energetic systems: concepts and applications of the PEGASE platform,” presented at the ECOS conference, Wroclaw, Poland, 2019.
[43] *IBM ILOG CPLEX Optimization Studio V12.7.0 documentation*. 2015.
[44] L. Giraud, R. Bavière, M. Vallée, and C. Paulus, “Presentation, Validation and Application of the DistrictHeating Modelica Library,” Versailles, France, 2015, p. 10.
[45] Free Software Foundation, Inc., “GNU Linear Programming Kit for GLPK Version 4.55,” Reference Manual, 2014.